

# Synthesis and Characterization of High Performance, Transparent Interpenetrating Polymer Networks With Polyurethane and Poly(methyl methacrylate)

S.A. Bird,<sup>1</sup> D. Clary,<sup>2</sup> K.C. Jajam,<sup>3</sup> H.V. Tippur,<sup>3</sup> M.L. Auad<sup>1</sup>

<sup>1</sup> Department of Polymer and Fiber Engineering, Auburn University, Alabama 36849

<sup>2</sup> Department of Chemistry and Biochemistry, Auburn University, Alabama 36849

<sup>3</sup> Department of Mechanical Engineering, Auburn University, Alabama 36849

Transparent, interpenetrating polymer network (IPN) materials were synthesized using polyurethane (PU) and poly(methyl methacrylate) (PMMA). PMMA contributed to the transparency and rigidity necessary for use in impact-resistant applications, whereas PU contributed to toughness. Several factors affecting the physical properties, such as the ratio of PU to PMMA, curing profile, inclusion of different isocyanates for the PU phase, and use of an inhibitor in the PMMA phase, were investigated. Full-IPNs were synthesized so that the two polymer networks would remain entangled with one another, and domain sizes of each system were reduced, mitigating phase separation. Both simultaneous IPNs, polymerization of monomers occurring at the same time, and sequential IPNs, polymerization of monomers occurring at different temperatures, were synthesized for studying the reaction kinetics and final morphologies. The phase morphology and the final thermal and mechanical properties of the IPNs prepared were evaluated. Findings suggest that samples containing ~80 wt% PMMA, 1,6-diisocyanatohexane 99+% (DCH), and an inhibitor with the MMA monomer created favorable results in the thermo-mechanical and optical properties. POLYM. ENG. SCI., 00:000-000, 2012. © 2012 Society of Plastics Engineers

## INTRODUCTION

Personal and public safety has always been a top priority, but with more innovative and sophisticated weapons, there is an increased demand for better protection. With both advanced munitions in the military in addition to everyday domestic hazards, creating a transparent material

that can allow ease of visibility as well as exhibit high strength and toughness is imperative in today's world. While several different methods of creating improved glass windows, such as bullet-resistant glass [1], have been studied and utilized in the past, other materials [2], especially polymers [3, 4], have also been explored for this purpose. An ideal polymeric material for applications such as windshields, windows, eye protection, and other situations where a strong, transparent material is desirable, should be flexible enough to absorb energy from an impact as well as sufficiently rigid to remain stable while in use [5].

Individual polymers are known to possess a wide range of characteristics that can be manipulated physically, thermally, and chemically. Furthermore, combining these materials into various mixtures can extend the ranges of properties offered by polymers [6]. A well established method of toughening plastics is the addition of a rubbery material into a polymeric matrix. This approach has been extensively reviewed in the polymer field [7-9]. In general, the morphologies of these materials consist of a continuous, highly stiff phase with a large number of dispersed, elastomeric domains. The current study focuses on synthesizing multicomponent interpenetrating polymer networks (IPN) with a high degree of optical transparency as well as good stiffness and toughness.

IPNs were first reported around 1914 when the chief chemist of Thomas Edison, Jonas Aylsworth, mixed a crosslinked phenol formaldehyde resin with rubber and sulfur for creating tougher phonograph records [10, 11]. Since this success, IPNs have been a popular subject, especially gaining recognition in the 1960s [10-12]. These unique materials are usually a combination of two or more polymers coexisting in a network form [13]. This article introduces several variations of IPNs, falling in between the classical sequential and simultaneous IPN syntheses.

Correspondence to: M.L. Auad; e-mail: auad@auburn.edu

Contract grant sponsor: Defense Threat Reduction Agency (DTRA); contract grant numbers: HDTRA 1-09-1-0023, BRBAA08-F-2-0104.

DOI 10.1002/pen.23305

Published online in Wiley Online Library (wileyonlinelibrary.com).

© 2012 Society of Plastics Engineers

When studying IPNs, it is vital to also investigate the degree of the crosslinked network present in the system. IPNs consisting of all polymer phases completely crosslinked are referred to as full-IPNs; whereas, IPNs with at least one phase not crosslinked are named semi-IPNs. Systems with no crosslinked phases are actually polymer blends [13]. Through ionic or covalent bonding of the resultant polymer phases, crosslinks can offer significant improvement of the physical properties, such as increased toughness, thermal stability, creep resistance, and elastic modulus [14].

Numerous techniques have been explored for finding the most effective and efficient IPN material that displays the best possible compatibility with minimal phase separation. If the phase that is synthesized first is too heavily crosslinked, there may not be enough room for the second polymer to swell and penetrate the first network, thus eventually creating two separate phases [15].

The purpose of this research was to create materials with comparable mechanical performance to impact-resistant glass or similar materials that could also be used for other applications. The full-IPN systems developed in this work were prepared by combining a soft, rubbery, high impact-absorbing PU phase with a highly stiff PMMA phase. A sequential interpenetrating network was formed where an elastomeric PU was polymerized first; following this, the PMMA phase, which was swelling the rubbery phase, was polymerized in situ within the PU network. During this study, the phase morphology and the final thermal and mechanical properties of IPNs were evaluated. In addition, a simultaneous IPN using the same reactants was studied, and the results were compared to the sequential IPN.

## EXPERIMENTAL AND TESTING PROCEDURES

### Materials

Two types of polyols were employed for the PU phase: 1,1,1-tris(hydroxymethyl) propane (TRIOI) from Acros Organics and poly(tetramethylene ether) glycol (PTMG) average  $M_n \sim 650 \text{ g mol}^{-1}$  from Sigma–Aldrich. The diol and triol were combined beforehand, through melting and mixing to ensure an equal dispersion of both types of polyols. The PTMG and TRIOI mixture was melted in an oven under a strong vacuum to remove moisture. In conjunction, the use of two different isocyanates was compared: 1,6-diisocyanatohexane 99+% (DCH) from Acros Organics and tolylene-2,4-diisocyanate 95% (TDI) from Sigma–Aldrich. The catalyst that was included for the reaction to take place was dibutyltin dilaurate, 98% (DD) distributed by Pfaltz & Bauer. Ethyl acetate was used as an analogue for DD.

For the PMMA phase, two versions of methyl methacrylate, 99% stabilized (MMA) from Acros Organics, were evaluated. The first version of MMA contained an inhibi-

tor, 10–20 ppm hydroquinone monomethyl ether (MEHQ). Additionally, another version of MMA monomer was prepared by removing the inhibitor through distillation. Both types of monomers were dried with molecular sieves to eliminate moisture. Trimethylolpropane trimethacrylate (TRIM) from Sigma–Aldrich was utilized as a crosslinker, and 2,2'-azobis(2-methylpropionitrile), 98% (AIBN) from Sigma–Aldrich was used as an initiator.

### Procedure

The IPN reaction was carried out in a one-step procedure. All reactants were mixed together at room temperature conditions, and no solvent was used during synthesis. First the PMMA system was prepared by mixing a MMA monomer, TRIM, and AIBN. After the components for the PU phase, the PTMG/TRIOI mixture and either DCH or TDI, were mixed separately, these were added to the PMMA precursor solution. Following this, DD was added to catalyze the PU system. After mixing these solutions, all samples were placed in the oven at 60°C for 24 h after which the temperature was raised to 80°C for an additional 24 h. The following ratios were used: PTMG to TRIOI (5.3:1.1 by mass), PTMG/TRIOI to DCH/TDI (1.8571:1 by mass), PTMG/TRIOI to DD (1 g:15.3846  $\mu\text{L}$ ), PMMA to TRIM (95:5 by mass), and 1.3 mL of AIBN (with ethyl acetate as an analogue) for every 123.5g of MMA.

One parameter investigated was the effect of different heat treatments on the IPN systems. Some IPNs were postcured in an oven an additional 2 h at 120°C so that changes in mechanical properties from different curing profiles could be studied. However, the additional curing produced a yellow coloration, decreased transparency, and did not affect the thermomechanical properties. It was thus decided that for further studies, postcuring would not be included.

As mentioned earlier, two different types of MMA monomers were used; one included an inhibitor while the other did not. The procedure for making an IPN was exactly the same as what was described earlier.

Following this synthesis, several IPN formulations were prepared. The ratio of PMMA to PU content varied from 80 wt% PMMA and 20 wt% PU to 40 wt% PMMA and 60 wt% PU. With these varying ratios, the use of TDI or DCH as well as the inclusion of the MMA monomer with or without an inhibitor also alternated.

### Characterization Techniques and Equipment

To obtain information on the mechanical and thermal properties of the IPNs, tensile testing and three-point bending tests were performed on a TA Instruments RSAIII dynamic mechanical analyzer (DMA) with a frequency of 1Hz. The thermal properties of the systems were observed using a TA Instruments Q2000 modulated differential scanning calorimeter (DSC).

Transparency was measured using a UV–visible 2450 spectrophotometer from Shimadzu Scientific Instruments.

Both a Zeiss EVO 50 variable pressure scanning electron microscope (SEM) with digital imaging and EDS (with the IPNs sputter-coated with an EMS 550X auto sputter coating device with carbon coating attachment) and a Zeiss EM 10C 10CR transmission electron microscope (TEM) were used to study the morphology of the IPNs.

The sample preparation technique used for the TEM was based on Kato's osmium tetroxide ( $\text{OsO}_4$ ) staining method [16]. These specimens were cut into small wedges and were allowed to sit in the dye for at least 48 h. Once sufficient dye had penetrated the materials, the samples were microtomed. When comparing the two polymer systems, PU absorbed the dye, becoming black, while PMMA remained unstained. This distinction between PMMA and PU enabled the study of the domain formation and phase separation processes for the IPN systems. Other research groups were also able to study the morphologies of their IPN systems based on this technique [17–19].

To characterize toughness of IPNs in terms of the critical-stress-intensity factor,  $K_{Ic}$ , quasi-static fracture tests were performed in accordance with the ASTM D5045 test method. Equation 1 was used, where  $f(a/W)$  is a dimensionless function of the ratio  $a/W$ ,  $a$  is the crack of length,  $W$  is the specimen height, and  $B$  is the thickness. For quasi-static fracture tests, the cured IPN sheets were machined into rectangular coupons of dimensions 80 mm  $\times$  20 mm  $\times$  8 mm. An edge notch of 6 mm in length was cut into the samples, and the notch tip was sharpened using a razor blade. The single edge notched bend, SENB, specimens were loaded in displacement control mode with a testing speed of 0.25 mm  $\text{min}^{-1}$ . The load vs. deflection data was recorded up to crack initiation and during stable crack growth, if any; the crack initiation toughness,  $K_{Ic}$  was calculated using the load ( $P$ ) at crack initiation. For each IPN category, at least three sets of experiments were performed at laboratory conditions. The mode-I stress intensity factor for a single edge notched bend (SENB) specimen loaded in three-point bending using the linear elastic fracture mechanics is given by,

$$K_{Ic} = \frac{Pf\left(\frac{a}{W}\right)}{B\sqrt{W}} \quad (1)$$

$$f\left(\frac{a}{W}\right) = \frac{3\frac{a}{W}\sqrt{\frac{a}{W}}}{2\left(1+2\frac{a}{W}\right)\left(1-\frac{a}{W}\right)^{3/2}} \times \left[1.99 - \frac{a}{W}\left(1 - \frac{a}{W}\right) \left\{2.15 - 3.93\left(\frac{a}{W}\right) + 2.7\left(\frac{a}{W}\right)^2\right\}\right]$$

## RESULTS AND DISCUSSION

### Network Morphology

The phase morphology of the two polymer components showed significant dependence on both the starting mate-

rials and reaction conditions. Figure 1 shows TEM photos of sections cut from stained IPN samples containing 80 wt% PMMA and 20 wt% PU with varying diisocyanates, DCH (Fig. 1a) and TDI (Fig. 1b), and MMA monomers with and without inhibitor (Fig. 1c and d). A TEM analysis of a PMMA sample (Fig. 1e) can also be seen for comparison. The PU phase absorbed the dye, thus appearing as a dark color, while the clear zones correlate to the PMMA phase.

Figure 1a and b shows that the networks are consistent with the interpenetration of the two polymers. A fine dispersion of the component polymer domains is observed throughout the entire sample. The domains do not have a clear shape, although they seem to be rather spherical. This observation is an indication of the interpenetration process that is produced at the molecular level.

The polymerization process followed by the PU and PMMA systems is known as a sequential interpenetration [8, 20, 21]. When a sequential IPN was formed, one of the monomers, in this case the MMA, TRIM, and the initiator, polymerized after the first polymer, PU. Initially, the MMA and TRIM monomers were swelling the crosslinked PU network, while at the end of the reaction process, the PMMA polymerized in situ. In other words, the continuous phase of the PU network was filled with domains of PMMA. Several factors affect this type of process, such as the gel-point of the PU system, the compatibility of the monomers, the growth of the polymers, and the ratio of the reactants. Less phase separated materials were created in this manner.

Babkina et al. [22] suggested that the sequential reaction of the IPN systems form considerable amounts of topological engagements between the two polymer chains, facilitating the compatibility of the components. In addition, the continuity of the PU phase plays a significant role in the development of the PMMA phase of the IPN as well as the resulting phase separation. The size of the PMMA regions is governed by how loosely or tightly the PU network crosslinks. A highly open PU network will permit larger regions of PMMA phases to form. A densely packed PU network consisting of interchain domains will allow smaller, but more, PMMA domains to fill the first network. Part of this study involved creating an IPN with 90 wt% PMMA and 10 wt% PU. However, this was unsuccessful as substantial phase separation was observed. The presence of excess PMMA caused the IPN to separate into distinct phases, producing a completely phase separated system. The PU component was insufficient to create a continuous network during the first part of the polymerization; therefore, the phases rejected each other even more and did not form interlocked systems.

For the current study, a different approach was investigated. MMA monomer with extracted inhibitor was used during the polymerization of the IPN system. Figure 1c and d shows the electron microscopy analysis of DCH- and TDI-based IPNs without inhibitors. By observing these images, it appears that using the MMA monomer without the inhibitor produced considerable changes in

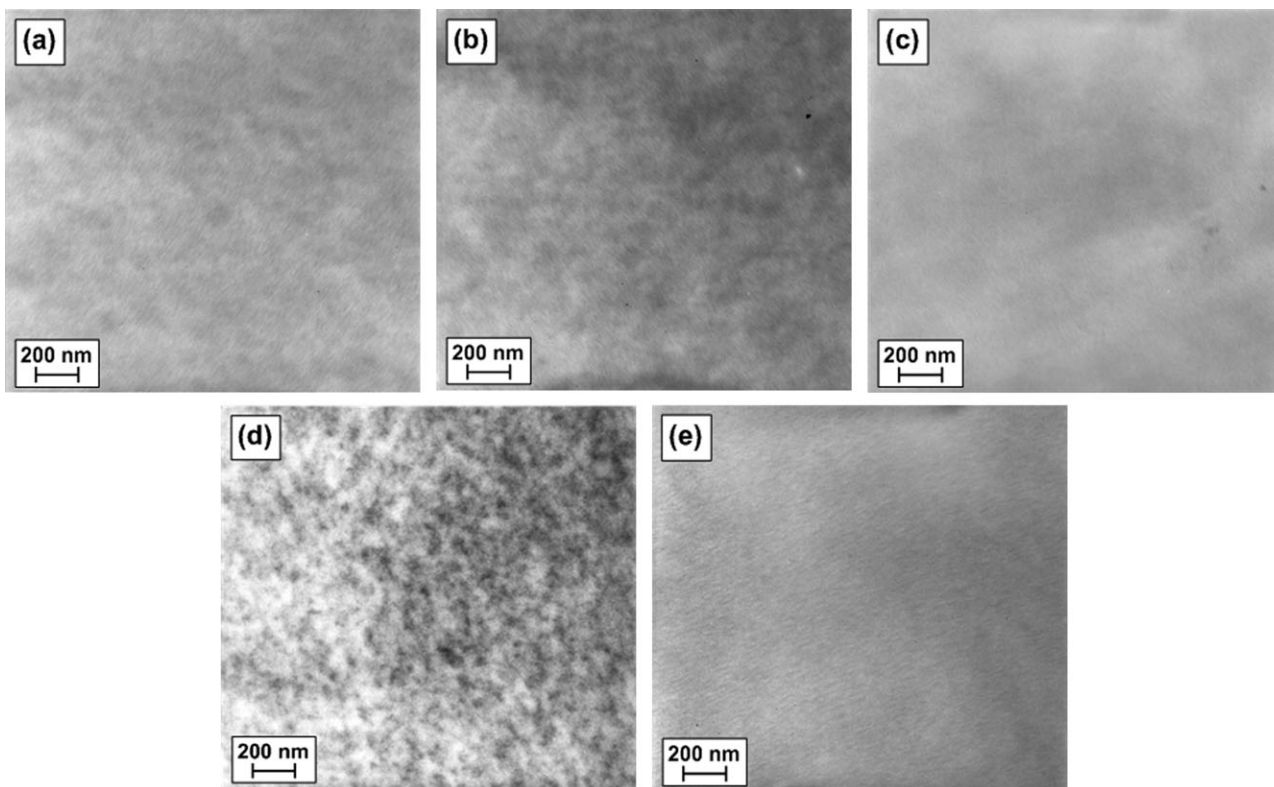


FIG. 1. TEM photos of IPNs with 80 wt% PMMA with (a) an inhibitor and DCH, (b) an inhibitor and TDI, (c) no inhibitor and DCH, (d) no inhibitor and TDI, and (e) pure PMMA with inhibitor.

the morphology of the IPN. In the absence of an inhibitor in the PMMA phase, the two polymers polymerized at the same time, thus producing a simultaneous IPN. This generated clear spherical domains (dark areas in the TEM photos), possibly due to incompatibility of the growing species during the polymerization process.

The kinetic and thermodynamic behavior plays a fundamental role in this reaction process. From these results, it is clear that the technique of successive curing of the two polymers is effective in enhancing the compatibility of the components in the system, thus allowing a lower degree of phase separation. Gelation of PU within the first 24 h of curing at 60°C was vital so that the PMMA would be contained in this network while polymerizing.

One approach in reaching a higher compatibility between the PU and PMMA phases in the IPN could be applying a higher pressure than that of ambient conditions. Lee et al. described using high pressure during synthesis for decreasing domain sizes, compared to using atmospheric pressure. The higher pressure made the two components more compatible with one another [19]. Using such an approach in the future may allow better compatibilization between the two phases in the current IPN system.

#### Degree of Transparency

Results from transparency analysis obtained on relatively thick samples (3.5 mm) were studied. Figure 2

summarizes UV–visible spectra corresponding to different IPNs containing 80 wt% PMMA and 20 wt% PU. It is important to note that the actual values of the samples should be higher because the light is reflected from each of the two surfaces encountered: on entering the sample, and on leaving. This is caused by the difference in refractive indices between the samples and air.

These results indicate that samples based on DCH or TDI present similar transmittance values (~82%). In addition, for samples not shown in this figure, all IPNs with

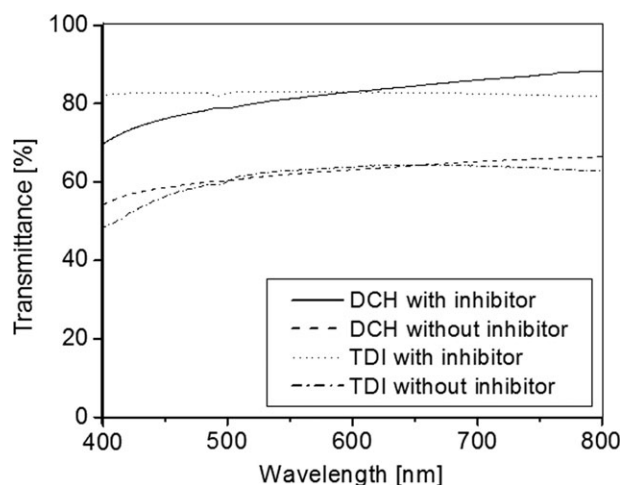


FIG. 2. UV–visible results showing IPNs consisting of 80 wt% PMMA and 20 wt% PU with different isocyanates.

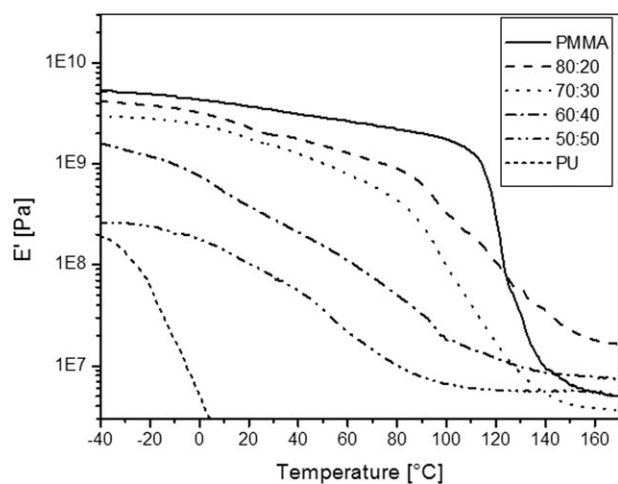


FIG. 3. DMA results showing change in  $E'$  for IPNs with various amounts of PMMA to PU content with DCH.

varying amounts of PMMA and PU from 40 to 80 wt% PMMA content had high transmittance values between 75 and 90%.

Visual inspections of the samples show that the aliphatic diisocyanate (DCH) produced clear samples, whereas the aromatic TDI created a drastic change in color, a dark yellow-orange. Some studies have suggested that the benzene ring in TDI contributes to this change in color. Rosu et al. reported that the yellowing of PU is due to UV radiation [23]. Yellowing is a result of photo-oxidation in the backbone chain through the aromatic ring by a quinoid path, leading to the degradation of PU and thus affecting the clarity and color of the material's surface [23].

On the other hand, samples without inhibitor in the monomeric MMA phase (simultaneous IPN) were studied, and the results are also shown in Fig. 2. These materials displayed less transparency than the counterpart produced with inhibitor (sequential IPNs). While samples containing an inhibitor displayed transparency between 70 and 90%, those that did not have the inhibitor showed transparency between 40 and 70%. This phenomena correlates to the morphology previously described, regarding the kinetics and phase separation process of the IPNs.

### Thermal and Mechanical Characterization

As mentioned earlier, several factors affected the kinetics of the IPN systems; this was evidenced in the thermo-mechanical response of the networks. The parameters studied in the present work included the ratio of PMMA to PU and the presence of an inhibitor in the monomeric MMA phase. However, other important factors were constantly maintained during the polymerization process, such as the ratio of di- to tri-functionalized monomers (PTMG/TRIOL for the PU phase and MMA/TRIM for the PMMA phase), which related the crosslink density of the two polymers. Other consistent parameters

were the amount of catalyzers utilized (DD and AIBN) as well as polymerization temperatures and time for the two-step reactions; and molecular weight of the PTMG and TRIOL utilized.

The most prominent effect in the thermo-mechanical properties was due to the variation of PMMA to PU ratio. Figures 3 and 4 show the dynamic mechanical properties (storage modulus,  $E'$ , and  $\tan \delta$ ) of DCH-based IPNs as a function of temperature. In addition, Table 1 summarizes the results for the different systems studied.

As expected, samples containing increasing amounts of PMMA exhibited a higher stiffness. The IPN consisting of 80 wt% PMMA showed a storage modulus close to 2 GPa at 30°C. Samples near 50 wt% PMMA showed lower values with regard to stiffness, which is associated to the contribution of the elastomeric PU phase.

The  $\tan \delta$  curves presented in Fig. 4 also demonstrate variation in the thermo-mechanical properties. A clear maximum peak in the  $\tan \delta$  curve shows the characteristic glass transition temperature,  $T_g$ , of the system and marks the temperature at which the network becomes rubbery in nature. This peak gained prominence with increasing proportions of PMMA and moved to considerably high temperatures. On the other hand, by increasing the amounts of the rubbery phase, this peak became broader, suggesting several relaxation mechanisms in the produced network. This may be associated with the nano/micro-domains produced when the relative amounts of the two phases were similar. A single peak in the  $\tan \delta$  curve also proves that we have considerable molecular mixing in the IPN.

The use of different isocyanates in the PU phase proved to also drastically change the dynamic mechanical properties. As seen in Table 1, IPN samples containing DCH possessed a much higher stiffness from those samples containing TDI. This was produced by the open conformation of the aliphatic isocyanate (DCH), which created a more open structure in the formation of PU chains. On the other hand, TDI (tolylene-2,4-diisocyanate)

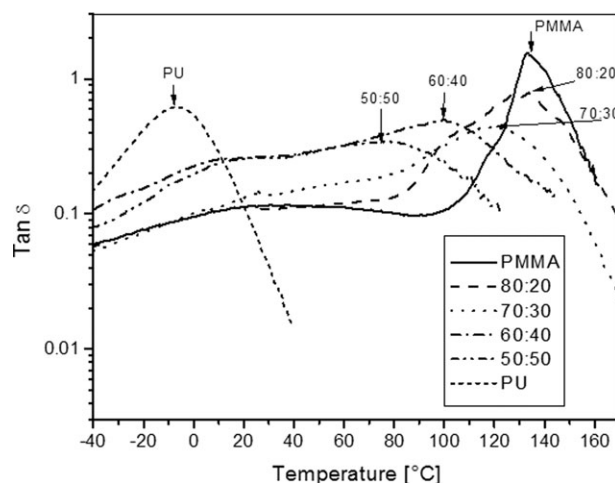


FIG. 4. DMA results showing change in  $\tan \delta$  for IPNs with various amounts of PMMA to PU content with DCH.

TABLE 1. IPNs with an inhibitor, and their respective wt% of PMMA and Young's modulus,  $E'$ , at 50°C;  $T_{g,s}$  were obtained from the maximum in  $\tan \delta$  curves.

Sample	wt% PMMA	$E'$ [Pa] at 50°C	$T_g$ (°C)
PMMA [24]	100%	$3.43 \pm 0.05 \times 10^9$	106
IPN with DCH	80%	$1.25 \pm 0.36 \times 10^9$	$125.10 \pm 7.63$
	70%	$0.23 \pm 0.06 \times 10^9$	$93.87 \pm 4.15$
	60%	$0.06 \pm 0.01 \times 10^9$	$70.60 \pm 0.34$
	50%	$0.03 \pm 0.01 \times 10^9$	$62.90 \pm 3.55$
IPN with TDI	80%	$0.22 \pm 0.02 \times 10^9$	$111.27 \pm 1.60$
	70%	$0.12 \pm 0.03 \times 10^9$	$70.62 \pm 7.78$
	60%	$0.10 \pm 0.01 \times 10^9$	$63.00 \pm 1.25$
	50%	$2.82 \times 10^6$	24.76

formed a curved structure with perhaps some incompatibilities in the network. Yang et al. [25] studied different diisocyanates in the production of shape memory polymers and observed similar results in the thermo-mechanical properties. Mishra et al. [26] compared aliphatic with aromatic PU samples. They concluded that the better proximity of the aliphatic polyurethane chain can form strong networks and ultimately generate large domains, responsible for improved PU properties.

As noted before, there were considerable changes in the thermo-mechanical properties of the IPNs due to the inclusion of an inhibitor in the PMMA phase. The  $\tan \delta$  results as a function of temperature, which can be seen in Fig. 5, reveal that there are two peaks in the  $\tan \delta$  curves for samples without an inhibitor (simultaneous IPN) versus only one peak for samples with inhibitor (sequential IPN). This was also true for the two systems based on DCH or TDI, and corresponded to two  $T_{g,s}$ , which indicated that phase separation did occur. If complete integration of the two systems was achieved, one peak would be observed, as in the curves for the samples with an inhibitor. This suggests that phase separation, if any, was less prominent in IPNs that followed a sequential polymerization instead of a simultaneous reaction.

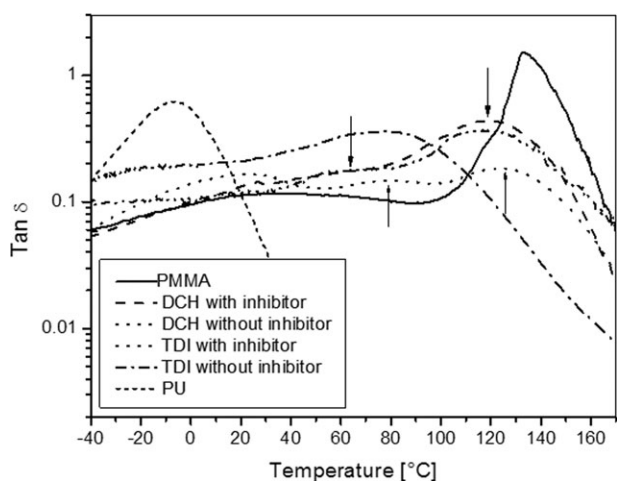


FIG. 5. Plots of  $\tan \delta$  versus temperature for IPNs with 80 wt% PMMA and 20 wt% PU content with DCH or TDI.

TABLE 2. Quasi-static fracture response ( $K_{Ic}$ ) for various IPNs with an inhibitor and DCH.

IPN (PMMA:PU)	Quasistatic fracture toughness $K_{Ic}$ (MPa m <sup>1/2</sup> )
100:0	$1.12 \pm 0.04$
90:10	$1.69 \pm 0.09$
85:15	$1.73 \pm 0.05$
75:25	$1.49 \pm 0.06$
70:30	$1.08 \pm 0.05$

### Fracture Properties

The quasi-static crack initiation toughness,  $K_{Ic}$  results for IPNs samples with DCH are shown in Table 2. An  $\sim 60\%$  improvement in static crack initiation toughness is quite evident for IPNs when compared to the neat PMMA. Furthermore, the trends in  $K_{Ic}$  values with increasing PU content suggest that there is an optimum PMMA/PU ratio for which the quasi-static fracture toughness is highest. In this work, 90/10 and 85/15 IPNs provide maximum fracture toughness among all cases.

### Surface Morphology

Another aspect of these IPNs that was studied involved the fracture mechanics at the microscale. For studying crack propagation, samples were broken at liquid nitrogen temperatures to create brittle failure and to avoid a temperature increase during fracture, especially above the  $T_g$ . This could have created a change in the morphology of the surface. Figure 6 shows the fractured surfaces of IPN samples with different PMMA to PU ratios. A commercial PMMA sample was included for comparative purposes.

Studying the SEM images, it appears that the more PU included in the IPN system, the more surface area was created and potentially more energy dissipated in the fracture process. These results correlate with the fracture properties presented in Table 2. These characteristics are essential for impact resistance; the higher degree of deformation energy a specimen can withstand, the less likely it will fail mechanically.

Phase separation was also affected by the ratio of PMMA to PU. When the PMMA concentration was  $>80$  wt%, the phases separated dramatically, affecting both mechanical and optical properties.

Samples with  $>40$  wt% of PU showed a clear plastic deformation typical of a rubbery phase, with areas of brittle failure interspersed. These separated areas could show signs indicative of a phase inversion process. Previous studies [17, 27] have demonstrated that there is a point where IPNs can undergo an inversion route, where the continuous phase between polymers converts from one polymer to the other. Figure 6d–f shows some evidence of phase inversion during the polymerization for the materials created during the current study.

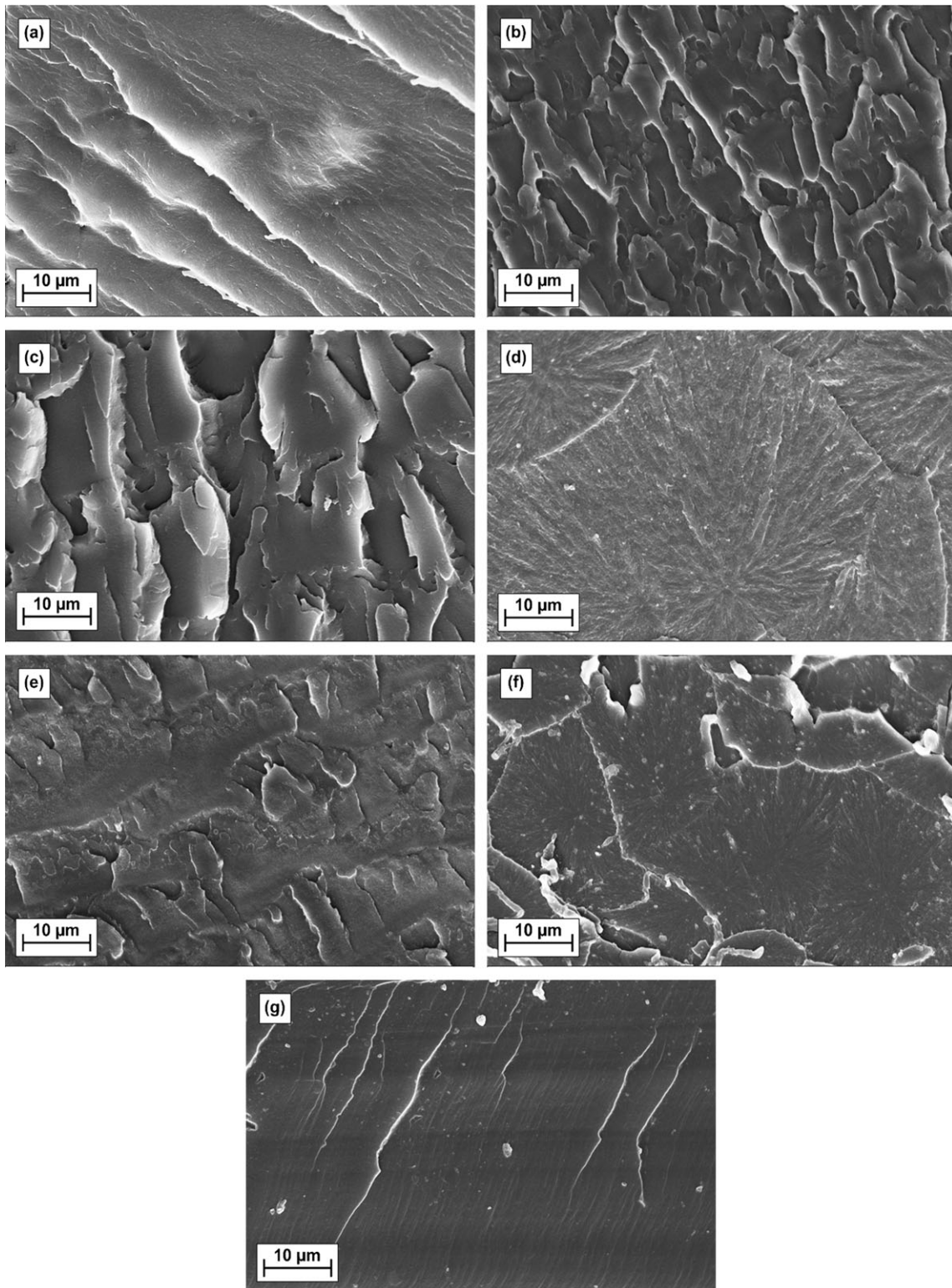


FIG. 6. SEM photos of (a) commercial PMMA; IPNs with an inhibitor and DCH: (b) 80 wt% PMMA, (c) 70 wt% PMMA, (d) 60 wt% PMMA, (e) 50 wt% PMMA, (f) 40 wt% PMMA, and (g) pure PU with DCH.

## CONCLUSIONS

This work reports the synthesis of full, interpenetrating polymer networks consisting of polyurethane and poly(methyl methacrylate). Several factors were studied, such

as the PU to PMMA ratio, the use of an inhibitor with the MMA monomer, and the inclusion of different isocyanates in the PU phase. After analysis of the effects of these parameters, it was concluded that samples with  $\sim 80$

wt% PU with the aliphatic structure of DCH, and also including the MMA monomer with an inhibitor, formed the best specimens. These materials displayed a high  $E'$  and  $T_g$ , a relatively high transparency, and the domain sizes of the phases were low with minimal phase separation. These systems show evidence as qualifiers for tough, energy-absorbing materials for engineering applications.

## REFERENCES

1. J.S. Amstock, *Handbook of Glass in Construction*, McGraw-Hill, New York (1997).
2. J. Rioux, C. Jones, M. Mandelartz, and V. Pluen, *Adv. Mater. Process.*, 31 (2007).
3. C. McLendon, A. Wakeling, C.B. Colby, H. Walton, and C. Grande, *Pop. Sci.*, **144**, 74 (1944).
4. P.J. Patel, G.A. Gilde, P.G. Dehmer, and J.W. McCauley, *AMPTIAC Newslett.*, **4.3**, 1 (2000).
5. C.E. Carraher and R.B. Seymour, *Seymour/Carraher's Polymer Chemistry*, CRC Press, New York (2003).
6. D. Klemmner, L.H. Sperling, and L.A. Utracki, *Interpenetrating Polymer Networks*, American Chemical Society, Washington, DC (1994).
7. Y. Huang, D.L. Hunston, A.J. Kinloch, and C.K. Riew, "Mechanisms of Toughening Thermoset Resins," in *Toughened Plastics I—Science and Engineering*, C.K. Riew and A.J. Kinloch, Eds., Advance in Chemistry Series 233, American Chemical Society, Washington, DC, 1 (1993).
8. A.J. Kinloch and F.J. Guild, "Predictive Modeling of the Properties and Toughness of Rubber-Toughened Epoxies," in *Toughened Plastics II, Novel Approaches in Science and Engineering*, C.K. Riew and A.J. Kinloch, Eds., Advances in Chemistry Series 252, American Chemical Society, Washington, DC, 1 (1996).
9. D. Verchère, H. Sauterau, J.P. Pascault, S.M. Moschiar, C.C. Riccardi, and R.J. Williams, "Rubber-Modified Epoxies," in *Toughened Plastics I—Science and Engineering*, C.K. Riew and A.J. Kinloch, ACS Advance in Chemistry Series 233, American Chemical Society, Washington, DC, 335 (1993).
10. C. Vasile and A.K. Kulshreshtha, *Handbook of Polymer Blends and Composites*, **3A**, Rapra Technology Ltd, Shawsbury (2003).
11. Y.S. Lipatov and T.T. Alekseeva, *Phase-Separated Interpenetrating Polymer Networks*, Springer, Berlin (2007).
12. D. Klemmner and K.C. Frisch, *Advances in Interpenetrating Polymer Networks*, **IV**, CRC Press, Lancaster (1994).
13. L.H. Sperling, *Polymeric Multicomponent Materials: An Introduction*, Wiley-Interscience, New York (1997).
14. L.H. Sperling, *Introduction to Physical Polymer Science*, Wiley-Interscience, New Jersey (2006).
15. Y. Zhi-zhong and E.M. Pearce, *J. Polym. Sci., Polym. Lett. Ed.*, **20.4**, 244 (1981).
16. K.J. Kato, *Polym. Sci. B*, **B4**, 35 (1966).
17. S.C. Kim, D. Klemmner, K.C. Frisch, W. Radigan, and H.L. Frisch, *Macromolecules*, **9.2**, 258 (1975).
18. G. Allen, M.J. Bowden, D.J. Blundell, G.M. Jeffs, J. Vyvoda, and T. White, *Polymer*, **14.12**, 604 (1973).
19. D.S. Lee and S.C. Kim, *Macromolecules*, 268 (1984).
20. G. Allen, M.J. Bowden, D.J. Blundell, F.G. Hutchinson, G.M. Jeffs, and J. Vyvoda, *Polymer*, **14**, 597 (1973).
21. J.C. Salamone, *Polymeric Materials Encyclopedia*, CRC Press, Boca Raton (1996).
22. N.V. Babkina, Y.S. Lipatov, T.T. Alekseeva, L.A. Sorochinskaya, and Y.I. Datsyuk, *Polym. Sci. Ser.*, **50.7**, 798 (2008).
23. D. Rosu, L. Rosu, and C.N. Cascaval, *Polym. Degrad. Stabil.*, 591 (2009).
24. J.E. Mark, *Polymer Data Handbook*, Oxford (1999).
25. J.H. Yang, B.C. Chun, Y.C. Chung, and J.H. Cho, *Polymer*, **44**, 3251 (2003).
26. A. Mishra, V.K. Aswal, and P. Maiti, *J. Phys. Chem. B*, **114**, 16 (2010).
27. S.C. Kim, D. Klemmner, K.C. Frisch, and H.L. Frisch, *Macromolecules*, **10.6** (1977).